Enhanced lifetime of Organic Photovoltaic diodes achieved by blending with PMMA: Impact of morphology and Donor:Acceptor combination

Balder A. Nieto Díaz[1], Christopher Pearson[1], Zakiya Al-Busaidi[1], Leon Bowen[2], Michael C. Petty[1] and Christopher Groves[1]*

[1]*Department of Engineering, Durham University, South Road, Durham DH1 3LE, United Kingdom*

[2]*Department of Physics, Durham University, South Road, Durham DH1 3LE, United Kingdom*

**email: chris.groves@durham.ac.uk*

ABSTRACT

In order to realise the potential of organic photovoltaic devices (OPVs) to provide cheap, scalable access to renewable energy, it is necessary to improve their lifetime and cost of encapsulation. The aim of this work is to achieve these aims by blending the donor and acceptor with the commodity polymer, PMMA, to form a ternary blend device with enhanced lifetime. We find that ternary OPV devices prepared in this manner can have up to double the lifetime of the binary control devices to an extent that depends upon the PMMA morphology and the processing additives used. Further, we find that the initial performance of ternary OPVs may decrease (in the case of PTB7-based blends) or slightly increase (in the case of P3HT-based blends) when compared to their binary counterparts, which is hypothesised to be due to donor compatibility with the PMMA. These findings suggest that this approach can be employed in other OPV blend systems and give design rules to maximise the positive impact on device lifetime.

Keywords:

1. Organic Semiconductors

2. Organic Photovoltaics

3. Lifetime

4. Aging

5. PMMA

Introduction

This paper addresses the need to improve the lifetime of organic photovoltaic (OPV) diodes through blending the donor:acceptor pair with an inert polymer, poly-methyl(methacrylate) (PMMA) which slows performance degradation via the 'gettering' of water [1]. Our contribution is twofold. We examine the impact of PMMA morphology on the effectiveness of this approach, thereby suggesting design rules for future devices. Additionally, we show that adding PMMA can be effective in extending the lifetime of more modern donor:acceptor pairs, although we also show that processing additives can have a detrimental impact. Taken together, these findings suggest a way forward to improving OPV lifetime that can be effective for a range of blend systems.

OPVs occupy an important space within the breadth of photovoltaic (PV) technologies. While future goals of installing terawatt (TW)-scale PV capacity is likely to be achieved when inorganic technologies can offer $0.5/W with lifetimes of 25 years [2], such devices may not be appropriate for all applications. In particular, flexible and light-weight PV panels may have a significant impact in the Global South where of the order of 1 Billion people do not have

reliable access to electricity and its allied advantages to health, education, productivity and income [3]. OPVs are a technology that may meet this need due to compatibility with scalable, roll-to-roll manufacture on flexible substrates [4] and the associated benefits of reduced cost [5]. Recent advances in donor, and particularly acceptor, materials have led to substantial improvements in the certified OPV record efficiency to 17.6% [6]. However, a significant remaining challenge in the commercialisation of OPVs is achieving an acceptable lifetime [7].

Although OPV devices combine a variety of donor and acceptor pairs with varying efficiencies, they degrade with similar mechanisms, which depend upon ambient light [8-10], temperature [11, 12], oxygen [13-15] and water [14, 16, 17]. Photo-oxidation of the donor polymer in particular impacts its electronic and mechanical properties [18], and although pairing the donor with the fullerene acceptors phenyl-C61-butyric acid methyl ester ($PC_{61}BM$) [19] and phenyl-C71-butyric acid methyl ester ($PC_{71}BM$) [20] improves photo-oxidative stability, it is not to a level where an acceptable lifetime is observed. Degradation of OPV performance is also accelerated by the presence of ambient water and oxygen [21], which can gain access to the active materials through microscopic pinholes in the electrode [22], whereupon they may react with the donor or acceptor [23] and lead to increased charge recombination [24]. While it is certainly the case that some donors and acceptors are more resistant to degradation than others [19, 25, 26], it is not yet the case that un-encapsulated OPV devices can achieve acceptable performance in ambient environments for several years. This in turn increases the importance of other methodologies to improve OPV lifetime. A variety of barrier layers that are compatible with flexible OPVs have been demonstrated, such as multilayers of parylene, Al_2O_3 and ZrO_2 [27-29] as well as fluorinated plastic laminates. However, these barriers do not yet provide sufficient protection from water vapour and oxygen to yield acceptable lifetimes and can also significantly inflate the cost [30-32] of the final device.

Al Busaidi et al. [1] recently demonstrated a new concept that reduces the rate at which OPV devices degrade. This involved combining the donor poly(3-hexylthiophene) (P3HT) and acceptor $PC_{61}BM$ with inert PMMA in a common solvent prior to deposition, and experiments showed that the ternary OPVs had longer lifetimes than the P3HT:$PC_{61}BM$ control to an extent which depended on the relative humidity, suggesting that the hygroscopic PMMA [33] acts as a gettering agent for water. Furthermore, and similar to Qin et al [34], they showed that the dilution of the donor:acceptor layer with PMMA actually slightly increased the power conversion efficiency (PCE), notwithstanding the lower P3HT:$PC_{61}BM$ content in the active layer. This approach of blending the donor and acceptor with PMMA is compatible with some encapsulation layers, and therefore may reduce the requirements placed on active materials and encapsulants for flexible and rigid OPV devices alike. However, two important questions remain unanswered: what role PMMA morphology plays upon the effectiveness of this approach; and is the technique applicable to other donor:acceptor blends? To address these issues, we report a series of experiments based on the donor:acceptor pairs P3HT:$PC_{61}BM$ and poly[[4,8-bis[(2-ethylhexyl)oxy]benzo[1,2-b:4,5-b']dithiophene-2,6-diyl][3-fluoro-2-[(2-ethylhexyl)carbonyl]thieno[3,4-b]thiophenediyl]] (PTB7):$PC_{71}BM$ in which the wt% and M_w of PMMA is varied. It is demonstrated that PMMA becomes more effective at extending OPV lifetime as PMMA phase separation becomes more pronounced. We ascribe this observation to water being more effectively contained within large PMMA domains as opposed to PMMA contained within the (largely) donor:acceptor matrix, and therefore suggests design rules for future OPV blends incorporating PMMA. It is also demonstrated that PMMA can enhance the lifetime of more highly performing PTB7:$PC_{71}BM$, albeit to a lesser extent than P3HT:$PC_{61}BM$, suggesting that blending PMMA could benefit the lifetime of a wide range of donor:acceptor blends. Finally, it is shown that the processing additive diiodooctane (DIO),

commonly used to optimise blend morphology, significantly limits the lifetime of OPV devices incorporating PMMA.

2. Experimental methods

2.1 OPV fabrication

Indium tin oxide (ITO) coated glass substrates were patterned into stripes by etching with zinc powder and hydrochloric acid, prior to sequential sonication for 15 minutes each in propanol-2-ol, acetone, Decon 90 solution (2% aqueous), and deionised water, followed by drying with N_2 gas. Cleaned substrates were treated with Oxygen plasma (Yield Engineering Systems Inc., YES-R3) for 5 min with 100W RF power. The conductive polymer poly(3,4-ethylenedioxythiophene):poly(styrene sulfonate) PEDOT:PSS (CLEVIOS P VP AI 4083) was filtered using a 0.2 μm poly(tetrafluoroethylene) (PTFE) syringe filter and spin-cast onto the substrate at 2500 rpm for 45s prior to annealing at 140 °C for 10 min in ambient atmosphere.

The polymer donors considered in this study were P3HT and PTB7, which were purchased from Rieke Metals and 1-Material Inc., respectively, alongside the acceptor fullerenes $PC_{61}BM$ and $PC_{71}BM$, purchased from 1-Material Inc. PMMA with molecular weights M_W =15 kg mol^{-1}, 97 kg mol^{-1} and 350 kg mol^{-1} were purchased from Sigma Aldrich. In all cases the materials were used as provided. Working in a N_2 glovebox, 30mg ml^{-1} solutions of the individual components were formulated. Details as to solvents used and stirring times are listed in Table S1 of the supplementary information. Two types of OPVs were fabricated, ternary OPVs containing a donor:acceptor and PMMA, and binary OPVs with only a donor and acceptor which served as a control. Binary solutions of P3HT:$PC_{61}BM$ were mixed in a 1:1 volume

ratio, while binary blends of PTB7:$PC_{71}BM$ were mixed in volume ratio of 1:1.5, and stirred overnight. Binary OPVs were fabricated by pipetting 150 µl of these mixtures onto the PEDOT:PSS coated substrates prior to spinning at 1000 rpm for one minute. Ternary OPVs were fabricated in a similar fashion by adding 30mg ml^{-1} solutions of PMMA to the binary solutions described above, prior to spin coating. In devices that use diiodooctane (DIO), this was added with a concentration of 3% to the binary or ternary solutions, and stirred for one hour before deposition. Detailed information about solvents used and stirring times are included in SI Table S1. Spin coating resulted in films of ~100nm thickness, whereupon ~150 nm of aluminium was thermally evaporated through a shadow mask. Finally, the devices were annealed at 120 °C for 10 min in the glovebox prior to testing.

2.2 Characterisation

The current-voltage characteristics of OPVs were measured in the dark and under AM 1.5 illumination (Oriel Sol1A 94021 A) using a Keithley 2400 SourceMeter. All measurements under illumination used a mask to restrict illumination to an active area of 0.79 mm^2. Each batch of OPVs comprised six substrates of four devices each that were measured to ensure reliable statistics. UV-vis absorption was measured alongside current-voltage measurements using a UV-1800 Shimadzu UV spectrophotometer. In all cases, we report measurements of typical devices rather than 'champion' devices with the highest performance or lifetime. Following initial characterisation in a N_2 atmosphere, OPVs were stored in a dark environmental chamber in ambient air with controlled temperature (20–25 ^oC) and humidity (40–50% RH), thereby following the standard of the International Summit on OPV Stability ISOS-D-1 shelf aging protocol [35]. Devices were removed from the environmental chamber for current-voltage and UV-vis absorption measurements to be taken, prior to being replaced for further aging. This process was repeated until the power conversion efficiency (PCE) fell

to 20% of its original value. AFM was used in a cleanroom environment to characterise surface topography and measure layer thicknesses. Gwyddion 2.50 image processing software [36] was used to analyse the characteristic surface features shown in the ternary OPV blends.

3. Results and discussion

3.1 Impact of PMMA morphology on OPV lifetime

To understand how the distribution of PMMA within the active layer effects OPV lifetime and performance, two series of ternary P3HT:$PC_{61}BM$:PMMA OPVs were manufactured in which both PMMA weight percent (wt%) and molecular weight (M_W) were varied. In this way, aspects of the ternary blend morphology could be controlled, and the corresponding impact on OPV performance measured. In one series, the wt% of PMMA with M_W of 350 kg mol^{-1} was increased from 5% to 15 wt%, while the other series had 15 wt% PMMA in which M_W was varied from 15 kg mol^{-1} to 350 kg mol^{-1}. Both series included binary P3HT:$PC_{61}BM$ OPV devices to serve as a control. Addition of PMMA to the binary blend led to the appearance of domed regions in the topology, as shown in Fig. 1a-d for the series of blend films in which PMMA M_W was varied. The corresponding AFM images for the series in which wt% of PMMA was varied are shown in the Supplementary Information (Fig. S1). Al-Busaidi et al. [1] also observed domed regions in the topology of P3HT:$PC_{61}BM$:PMMA OPVs with 14wt% of PMMA with M_W = 97 kg mol^{-1}. They used conductive AFM to show that domed regions had low conductivity when compared to the regions in-between, inferring that the former were PMMA-rich while the latter were P3HT:$PC_{61}BM$ rich. Here, we investigate the domed regions further using cross-sectional SEM, shown in Fig. 1e. Surprisingly, it is found that the PMMA-rich domains form *beneath* the active layer, suggested to be due to the high wettability of the PMMA on the PEDOT:PSS surface [37]. Given that the addition of PMMA extends the

lifetime of P3HT:PC_{61}BM-based OPVs in the presence of atmospheric water vapour [1], this suggests that atmospheric water has significant mobility in the device prior to reacting with the active materials, be it either through the PEDOT:PSS layer or through the P3HT:PC_{61}BM-rich active layer. This supposition is supported by conductive AFM images of ternary devices reported by Al-Busaidi et al. [1], since the conductivity of the P3HT:PC_{61}BM-rich regions degrades uniformly across the inhomogeneous film.

AFM studies on the present series of P3HT:PC_{61}BM:PMMA devices show that the size of the PMMA-rich domains can be controlled by the M_W and wt% of PMMA. Fig 1 shows that the size of the PMMA-rich domains increases with PMMA M_W for a constant wt% of PMMA (Supplementary Information Table S2 lists average area, density, and height of the PMMA-rich domes). We attribute the behaviour shown in Fig. 1 to PMMA dropping out of solution at an earlier point during the drying process as M_W increases, in turn leading to larger PMMA-rich domains and less PMMA in the otherwise P3HT:PC_{61}BM-rich regions, therefore resulting in a total higher volume of isolated PMMA (Fig. S2) that provides increased protection against water vapour. Fig. S1 shows that increasing wt% of PMMA whilst keeping the M_W constant for P3HT:PC_{61}BM:PMMA devices leads to increasing size of PMMA-rich domains. Unlike the first series, changing only the wt% of PMMA and not the M_W, is not expected to change the equilibrium concentration of PMMA in the PMMA-rich and P3HT:PC_{61}BM-rich regions [38]. The change in size of PMMA-rich regions is instead attributed to the greater availability of PMMA in solution. Hence, the two series of P3HT:PC_{61}BM:PMMA devices allow for some degree of control over the amount and whereabouts of PMMA within the OPV.

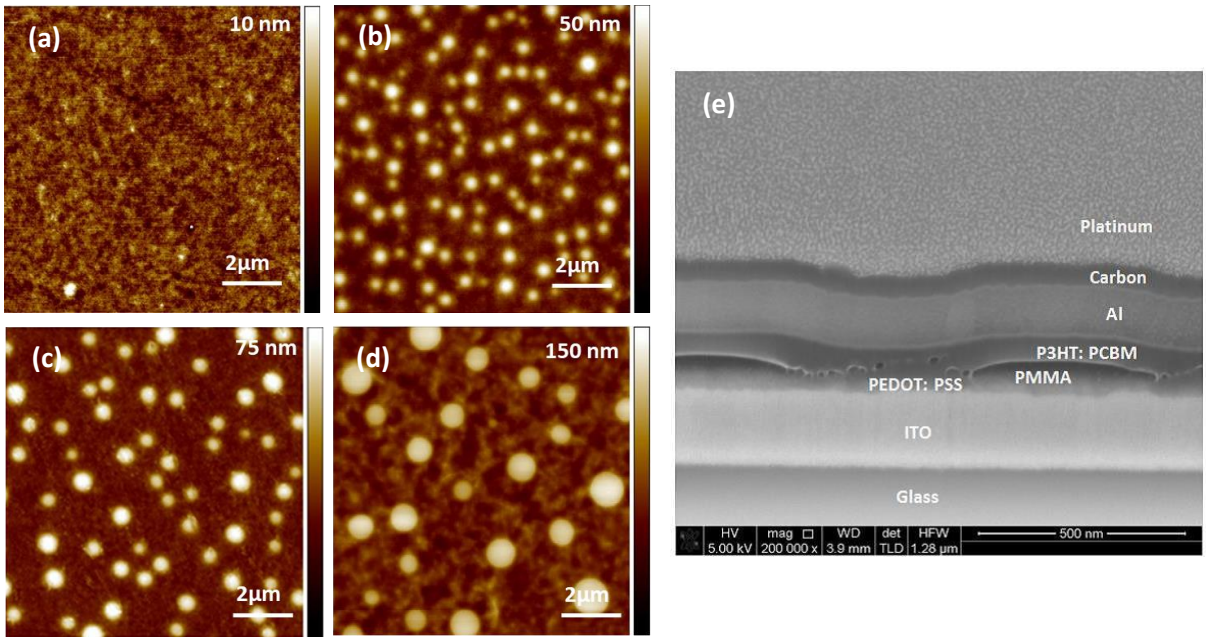

Figure 1: AFM topography images of active layers comprising (a) P3HT:$PC_{61}BM$ and P3HT:$PC_{61}BM$:PMMA with 15 wt% PMMA of M_W (b) 15 kg mol^{-1}, (c) 97 kg mol^{-1} and (d) 350 kg mol^{-1}. (e) Cross-sectional SEM image of a P3HT:$PC_{61}BM$:PMMA blend film with 14 wt% of M_W = 97 kg mol^{-1} PMMA.

We now turn our attention to the lifetime of the ternary OPVs. Fig. 2a illustrates ISOS-D-1 degradation of the PCE for typical P3HT:$PC_{61}BM$:PMMA OPVs with 15 wt% PMMA but varying M_W, normalised to the initial value. Similar to Al-Busaidi et al [1], it is shown that ternary OPVs with PMMA have a longer lifetime than the binary control. Fig. 2b-d shows that this improvement in lifetime is largely due to an improvement of the rate in which J_{SC} degrades when PMMA is introduced. The Fill Factor (FF) is shown to degrade slightly more slowly in presence of PMMA, whilst the open-circuit voltage (V_{OC}) stays largely constant for all devices with measurable photovoltaic action. It has been argued that the presence of water in P3HT:$PC_{61}BM$ OPV active layers leads to trap formation and increased recombination [24], and in turn, Al-Busaidi [1] argued that water-related trap-formation was slowed in the presence of PMMA. Data for other OPV systems suggest that increased trapping can lead to increased charge recombination [39, 40], in turn effecting J_{SC} and FF as seen here, hence our data is consistent with this explanation.

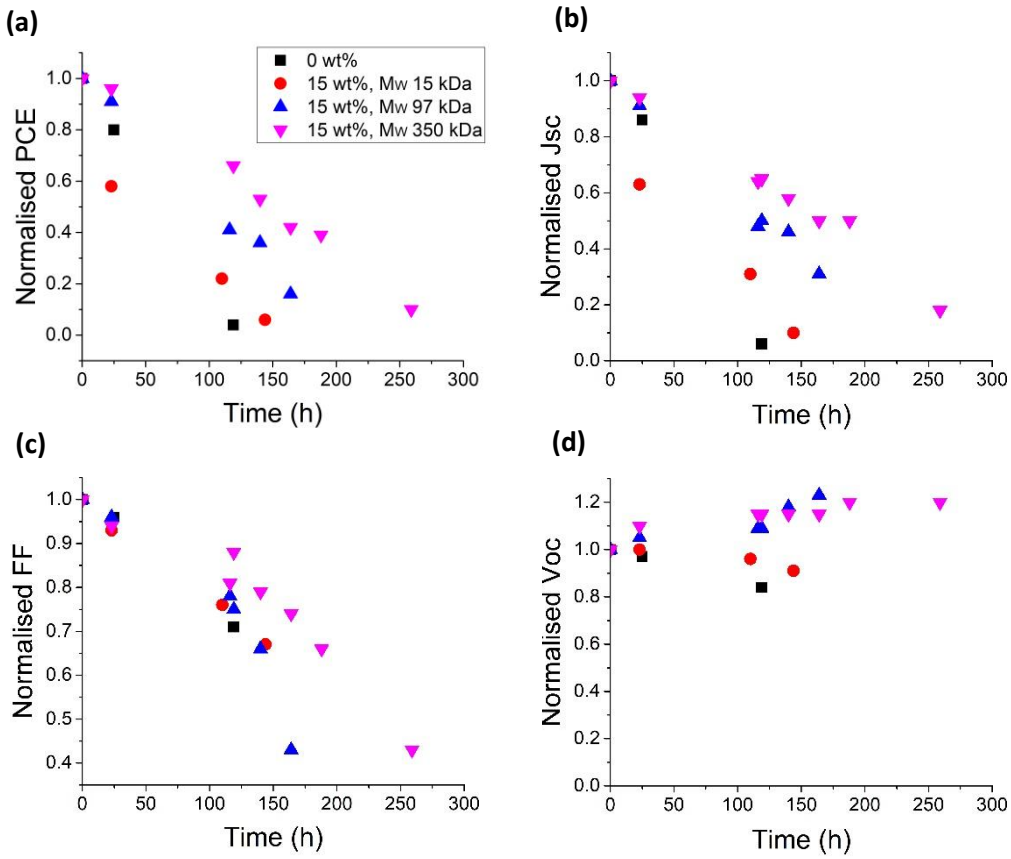

Figure 2: Normalised (a) PCE, (b) J_{SC}, (c) FF and (d) V_{OC} as a function of time for typical binary P3HT:$PC_{61}BM$ blend (black squares) and ternary P3HT:$PC_{61}BM$:PMMA blend with 15 wt% of PMMA and M_W = 15 kg mol^{-1} (red circles), 97 kg mol^{-1} (blue up triangles) and 350 kg mol^{-1} (pink down triangles). Devices were aged according to ISOS-D-1 standard.

Fig. 2a shows a significant variation in OPV lifetime upon PMMA M_W. We reiterate that this series of devices contain the same weight of PMMA, but that its distribution varies with M_W (Fig. 1). Surprisingly, it is shown that the beneficial effects of PMMA are most pronounced for the largest M_W (350 kg mol^{-1}), which have the largest, most widely spaced PMMA-rich regions (Fig 1d). Fig. S3c in the Supplementary Information shows normalised PCE lifetime for the second series of OPVs in which wt% of 350 kg mol^{-1} PMMA was increased from 0% to 15%. It can be seen that lifetime improves with increasing wt% of PMMA, which from Fig. S1, is associated with larger PMMA-rich domains. Supplementary Information Fig. S4 shows the improvement in lifetime is again largely due to a reduction in the rate at which J_{SC} degrades. Taken together, these data imply that large, widely-spaced PMMA-rich regions are most

effective at extending OPV lifetime, thus providing design criteria for future ternary OPV devices.

While the benefits of PMMA to OPV lifetime, as well as the role of morphology in this action, is demonstrated by the data, the precise mechanism by which PMMA extends lifetime in OPVs is less clear. We will, however, review the evidence thus far. Al-Busaidi et al [1] demonstrated that adding PMMA to P3HT:$PC_{61}BM$ slowed the rate of OPV degradation resulting from atmospheric water vapour. The route of water ingress could be through pinholes in the Al electrode [41] or diffusion through the PEDOT:PSS layer. While no pinholes could be observed in the Al electrodes following fabrication, localised delamination in the form of bubbles was observed following aging as shown in Supplementary Information Fig. S5. Luo et al [42] observed similar bubbles on the cathode of organic LEDs following aging in ambient air. This was argued to be due to the creation of Hydrogen gas by reaction between water and Aluminium, which in turn led to delamination of the electrode [43]. Further, Luo et al [42] found that PEDOT:PSS facilitated the formation of bubbles in the electrode, suggesting that the hygroscopic nature of PEDOT:PSS transported atmospheric water laterally through the device. We note that while both aged ternary and binary OPV devices showed bubbles on the Al electrode, the population of bubbles was reduced for the ternary device. Hence, our data appear to be consistent with initial atmospheric water ingress through the PEDOT:PSS, which is further accelerated by rupturing of the electrode due to reaction between Al and water. This process appears to be slowed by the presence of PMMA in the ternary blend. Combined with the physical process of electrode delamination is the change in opto-electronic properties of the active layer with aging. The present data show that degradation in PCE is primarily due to changes in FF and J_{SC}, which is indicative of an increase in recombination with aging. These data are consistent with shallow trapping (not recombination-active), as V_{OC} is minimally

affected as can be seen in Fig. 2d. It has been demonstrated that shallow traps can originate from clusters or simple traces of water [44, 45], which limits charge transport and increase the voltage dependence of current [44]. This is supported by Al-Busaidi et al [1], who argued that reduction in conductivity as measured by conductive AFM was due to increased trapping, itself due to chemical changes in the active layer with aging. Interestingly, however, they also showed that the there was little spatial dependence in the degradation of conductivity, despite the heterogeneity of the ternary film. Nonetheless, it seems that chemical changes in both the active layer and the electrode due to atmospheric water vapour play a role in degradation of PCE in P3HT:$PC_{61}BM$ OPVs. What seems more clear is that water has significant mobility in the active layer prior to interacting with the donor, acceptor, or electrode, and that during this mobile period, water can become trapped in the larger PMMA-rich domains, which in turn extends OPV lifetime.

Having established that PMMA can reduce the rate at which PCE degrades, we now turn to consider the impact of PMMA on initial absolute performance. Figures S6 and S7 in the Supplementary Information show the impact of varying wt% and M_W of PMMA respectively upon the statistics of PCE, J_{SC}, V_{OC} and FF. No significant trend in PCE is observed in either series, with most devices displaying a PCE in the region of 0.8 to 1.2%. We did however observe, as shown in Supplementary figure S8, that reverse leakage current reduces with addition of PMMA which we ascribe to a reduction in parallel current paths through the PMMA-rich regions shown in Fig. 1e. The reduction in reverse leakage current indicates that blending donor:acceptor materials with PMMA may also improve the detectivity of organic photodetectors [46]. These data add to those reported for organic field-effect transistors [47] and light-emitting diodes [48], which show that devices incorporating inert polymers can have similar or superior performance compared to those with all-conjugated active layers.

3.2 Impact of donor:acceptor system on effectiveness of PMMA

We now turn our attention to whether incorporating PMMA into the active layer can increase the lifetime of donor:acceptor systems. For this investigation a series of OPVs were fabricated with PTB7 as donor and $PC_{71}BM$ as acceptor, being an OPV blend with different morphological characteristics [49] and higher performance [50] than P3HT:$PCB_{61}BM$. The additive DIO is commonly used in binary PTB7:$PC_{71}BM$ OPVs to limit the size of fullerene aggregates and thereby maximise PCE [49, 51], hence, we begin by considering binary PTB7:$PC_{71}BM$ and ternary PTB7:$PC_{71}BM$:PMMA OPVs incorporating DIO as described in section 2.1. Fig. 3a shows ISOS-D-1 PCE degradation for ternary PTB7:$PC_{71}BM$:PMMA OPVs with 15 wt% of PMMA having M_W = 15, 97 and 350 kg mol^{-1}, compared to a binary PTB7:$PC_{71}BM$ OPV control. It is apparent that the lifetime of PTB7:$PC_{71}BM$-based devices is lower than that of P3HT:$PCB_{61}BM$ (Fig. 2), and that addition of PMMA has no discernible impact on OPV lifetime. Furthermore, Fig. S9 of the Supplementary Information shows that J_{SC} and PCE for ternary PTB7:$PC_{71}BM$:PMMA OPVs is less than half that of the binary counterpart.

We investigate the underpinning reasons for this further by looking at the morphology of the binary and ternary films. When adding PMMA to the PTB7:$PC_{71}BM$ films, domed regions were observed which increased in size as the M_W of the PMMA used was increased (Fig. 4), as was seen for P3HT:$PCB_{61}BM$:PMMA ternaries shown in Fig. 1. The impact of PMMA on the film morphology is therefore outwardly similar in the cases of both P3HT:$PCB_{61}BM$:PMMA and PTB7:$PC_{71}BM$:PMMA, making it unlikely that morphology is the reason for the difference in behaviour.

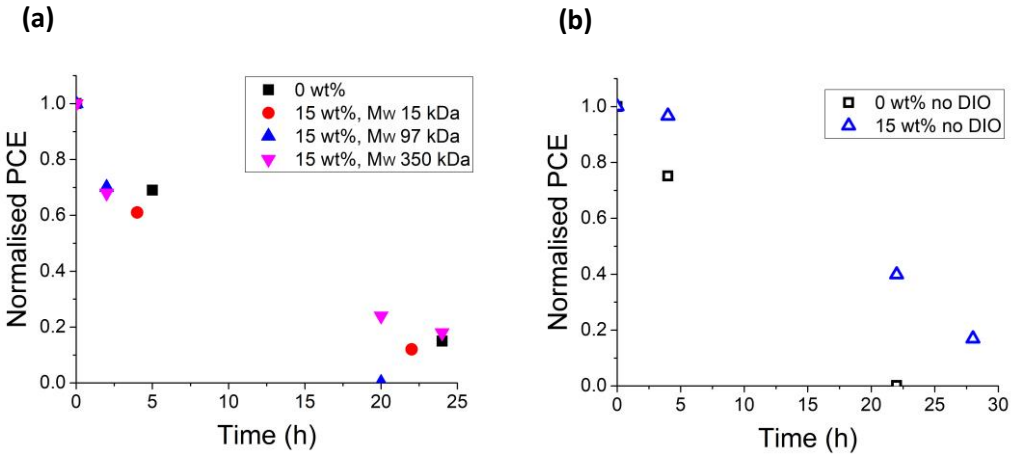

Figure 3: (a) Normalised PCE as a function of time for typical binary PTB7:$PC_{71}BM$ blend with DIO (black squares) and ternary PTB7:$PC_{71}BM$:PMMA blend with DIO and 15 wt% of PMMA and M_W = 15 kg mol^{-1} (red circles), 97 kg mol^{-1} (blue up triangles) and 350 kg mol^{-1} (pink down triangles). (b) Repeat of data shown in part 'a' without use of DIO, binary blend (open black squares) and ternary blend with 15 wt% of PMMA and M_W = 97 kg mol^{-1} (open blue up triangles). All devices were aged according to ISOS-D-1 standard.

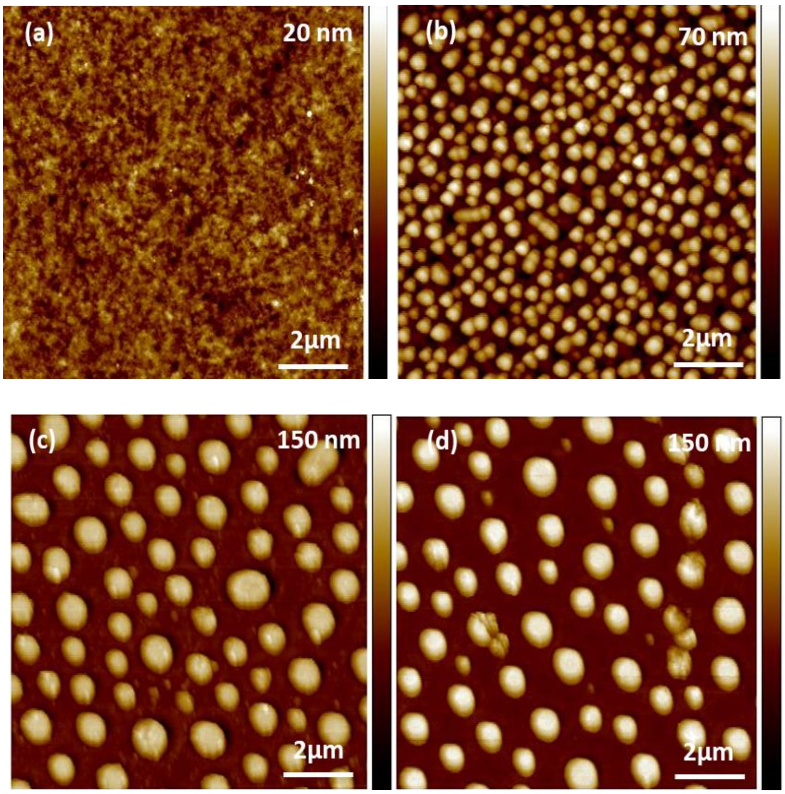

Figure 4: AFM topography images of (a) PTB7:$PC_{71}BM$, and of PTB7:$PC_{71}BM$:PMMA with 15 wt% of PMMA with (b) 15, (c) 97 and (d) 350 kg mol^{-1}.

One significant difference between the PTB7-based and P3HT-based devices is the use of DIO in the former. It has been shown that the use of processing additives can lead to increased photo-bleaching [52]. Therefore, we hypothesise that the poor lifetime of PTB7:$PC_{71}BM$:PMMA ternary OPVs may be due to residual DIO which becomes trapped in the PMMA. We tested this assertion by fabricating further PTB7:$PC_{71}BM$ and PTB7:$PC_{71}BM$:PMMA OPVs without DIO, and subjecting them to the same ISOS-D-1 aging protocol, as shown in Fig. 3b. It can be seen that incorporating PMMA in the PTB7:$PC_{71}BM$ blend when DIO is absent improves lifetime, thereby recovering the result seen for the P3HT-based devices, however, it is noted that improvement is less pronounced. More specifically, the length of time taken to drop to 20% of the initial PCE is improved by up to a factor of ~2 for P3HT-based blends when PMMA is added, whilst the corresponding improvement in lifetime for PTB7 based blends when PMMA is added is ~1.3. There are a number of possible reasons for this difference in behaviour. PTB7 contains a bridging O atom [52] which is not present in P3HT, and thus P3HT devices are more stable than their PTB7 counterparts. [53]. Further, PTB7-based devices were fabricated with $PC_{71}BM$, while P3HT with $PC_{61}BM$. The larger size of $PC_{71}BM$ has an influence on phase segregation in the polymer–fullerene blend films [54], which can lead to morphological changes with the passage of time, and may be one of the reasons for the poor ISOS-D-1 stability of $PC_{71}BM$-based devices [55]. The evidence that PMMA can extend the lifetime of PTB7:$PC_{71}BM$ OPVs, albeit slightly, suggests that water plays some role in these degradation mechanisms.

We note that the PTB7:PC71BM:PMMA OPVs with or without DIO show a decrease of >50% in initial JSC and PCE when compared to their binary counterparts (Figs. S9 & S10), indicating that PTB7-based devices initial performance is significantly affected by the addition of PMMA, contrary to P3HT-based devices, which are almost unaffected as described in the previous section. Fig. S15 in the Supplementary Information shows a decrease of ~24% in absorption of

P3HT:PC61BM:PMMA OPVs when compared to the binary control devices, while Fig. S19 shows a similar decrease of ~17-22% in absorption of PTB7:PC71BM:PMMA OPVs when compared to their binary counterparts, suggesting that changes in absorption are not the root cause of the difference in initial behaviour. Instead, we suggest that the differing impacts of PMMA upon initial performance of PTB7-based and P3HT-based devices is due to differences in microstructure. A previous study by Masataka Kumano et al., [56], used time resolved microwave conductivity (TRMC) to show that adding an insulating molecule as a ternary component can enhance photoconductivity in crystalline polymers like P3HT and PffBT4T, and degrade photoconductivity in amorphous polymer PTB7, in turn suggesting that insulating molecules/polymers are more compatible with crystalline than amorphous polymers. In other studies, energy filtered transmission electron microscopy (EFTEM) measurements have shown that P3HT:PC61BM films form nano fibrils; while there are no obvious PTB7 crystals in the PTB7:PC71BM films, only PC71BM aggregates [57, 58]. These data suggest that the addition of insulating polymers/additives can disrupt charge transport in PTB7:PC71BM:PMMA OPVs [59, 60]. This provides a deeper understanding of how inert polymers may be utilised within OPV devices, as our data suggest that PMMA can be effective in enhancing lifetime in multiple blend systems, but that it can also disrupt charge transport in amorphous donor polymers.

We now return to investigate the unfavourable impact of DIO upon lifetime in ternary OPVs. To that end, further P3HT:$PC_{61}BM$ based devices were fabricated with DIO, i.e. repeating experiments shown in Fig. 2 with DIO for comparison. Fig. 5 shows ISOS-D-1 degradation of PCE for binary P3HT:$PC_{61}BM$ OPVs and ternary P3HT:$PC_{61}BM$:PMMA OPVs comprising 15 wt% of PMMA with M_W = 97 kg mol^{-1}, both of which included DIO as an additive. The addition of PMMA to the blend leads to very rapid reduction of OPV performance as compared to the binary control, which is the opposite behaviour to that observed in P3HT:$PC_{61}BM$ based devices when DIO is absent (Fig. 2). We conclude that whilst incorporating PMMA as a

ternary component can improve lifetime in a range of donor:acceptor systems, its efficacy varies and is negatively impacted by use of some processing additives. We note that some studies have shown that washing the active layer with a small amount of an inert solvent with a low boiling point like methanol or ethanol can remove residual DIO and thus improve stability [61, 62]. This approach was tested on the current devices to examine whether it could reduce or remove the negative impact of DIO on ternary OPVs but were found to be ineffective. The results of these experiments are presented in Supplementary Information Fig. S16-19.

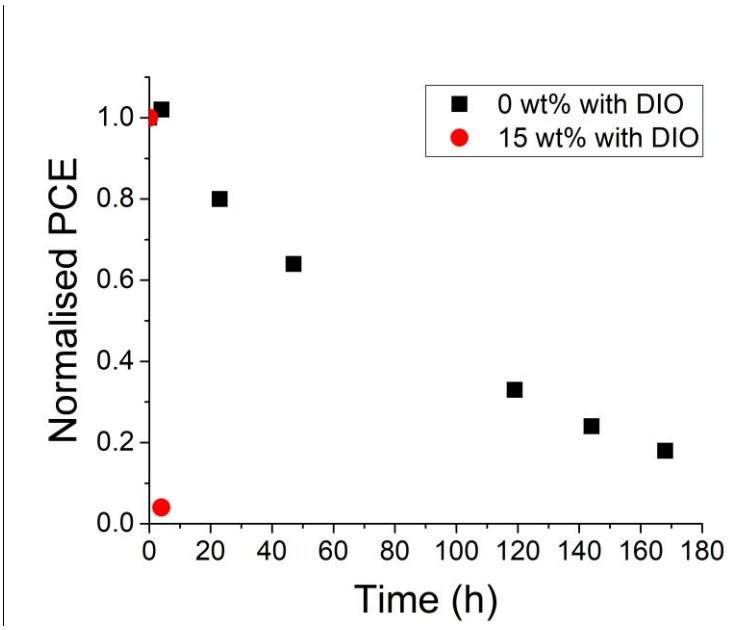

Figure 5: Normalised PCE as a function of time for typical binary P3HT:$PC_{61}BM$ blend (black squares) and ternary P3HT:$PC_{61}BM$:PMMA blend with 15 wt% and a 97 kg mol^{-1} (red circles), both of which were processed with DIO.

4. Conclusions

The commercial viability of OPV devices requires improvements in lifetime and a reduction in cost of encapsulant technologies. This paper has shown that the ISOS-D-1 lifetime of OPVs can be improved by forming a ternary blend between the donor and acceptor with PMMA. The improvements in lifetime were as high as a factor of 2 without significantly effecting power conversion efficiency of P3HT-based devices, while a lesser factor of 1.3 and an initial PCE drop of >50% was observed for PTB7-based devices. This shows that adding an inert polymer is more effective in some blend systems than in others, which is hypothesised to be due to the compatibility between the donor polymer and PMMA. Furthermore, our data show that the improvement in lifetime is sensitive to the PMMA morphology, with larger, PMMA-rich domains providing the most benefit, thereby providing design rules for future devices. As a final cautionary note, we also show how the use of processing additives (here DIO) in addition to PMMA can have a negative impact on lifetime, indicating some limitations to the processing methodologies for ternary OPV devices with PMMA.

Acknowledgements

We gratefully acknowledge CONACyT-SENER for the award of a scholarship (BND) (625176) and North East Centre for Energy Materials (NECEM) (EP/R021503/1) for additional funding, as well as Dr Richard Thompson (Durham University, Department of Chemistry) and the Durham Energy Institute for useful discussions.

References

[1] Z. Al-Busaidi, C. Pearson, C. Groves, M.C. Petty, Enhanced lifetime of organic photovoltaic diodes utilizing a ternary blend including an insulating polymer, Solar Energy Materials and Solar Cells, 160 (2017) 101-106.
[2] N.M. Haegel, R. Margolis, T. Buonassisi, D. Feldman, A. Froitzheim, R. Garabedian, M. Green, S. Glunz, H.-M. Henning, B. Holder, I. Kaizuka, B. Kroposki, K. Matsubara, S. Niki, K. Sakurai, R.A. Schindler, W. Tumas, E.R. Weber, G. Wilson, M. Woodhouse, S. Kurtz, Terawatt-scale photovoltaics: Trajectories and challenges, 356 (2017) 141-143.
[3] S. Foundation (2019). "Access to energy is the bedrock of inclusive economic growth." Accessed 17-May, 2019, from https://shellfoundation.org/focus-areas/access-to-energy/.
[4] F.C. Krebs, T. Tromholt, M. Jørgensen, Upscaling of polymer solar cell fabrication using full roll-to-roll processing, Nanoscale, 2 (2010) 873-886.
[5] I. Report (2012). "Renewable Energy Cost analysis – Solar Photovoltaics." Accessed 20-Sep, 2018, from https://www.irena.org/-/media/Files/IRENA/Agency/Publication/2012/RE_Technologies_Cost_Analysis-SOLAR_PV.pdf.
[6] Q. Liu, Y. Jiang, K. Jin, J. Qin, J. Xu, W. Li, J. Xiong, J. Liu, Z. Xiao, K. Sun, S. Yang, X. Zhang, L. Ding, 18% Efficiency organic solar cells, Science Bulletin, 65 (2020) 272-275.
[7] Y. Zhang, I.D.W. Samuel, T. Wang, D.G. Lidzey, Current Status of Outdoor Lifetime Testing of Organic Photovoltaics, Adv Sci (Weinh), 5 (2018) 1800434.
[8] M. Manceau, S. Chambon, A. Rivaton, J.-L. Gardette, S. Guillerez, N. Lemaître, Effects of long-term UV–visible light irradiation in the absence of oxygen on P3HT and P3HT:PCBM blend, Sol. Energy Mater. Sol. Cells, 94 (2010) 1572-1577.
[9] J. Razzell-Hollis, J. Wade, W.C. Tsoi, Y. Soon, J. Durrant, J.-S. Kim, Photochemical stability of high efficiency PTB7:PC70BM solar cell blends, J. Mater. Chem. A, 2 (2014) 20189-20195.
[10] A. Rivaton, A. Tournebize, J. Gaume, P.-O. Bussière, J.-L. Gardette, S. Therias, Photostability of organic materials used in polymer solar cells, Polymer International, 63 (2014) 1335-1345.
[11] M. Manceau, A. Rivaton, J.-L. Gardette, S. Guillerez, N. Lemaître, The mechanism of photo- and thermooxidation of poly(3-hexylthiophene) (P3HT) reconsidered, Polym. Degrad. Stab., 94 (2009) 898-907.
[12] Y. Zhang, H. Yi, A. Iraqi, J. Kingsley, A. Buckley, T. Wang, D.G. Lidzey, Comparative indoor and outdoor stability measurements of polymer based solar cells, Sci Rep, 7 (2017) 1305.
[13] A. Tournebize, P.-O. Bussiere, A. Rivaton, J.-L. Gardette, H. Medlej, R.C. Hiorns, C. Dagron-Lartigau, F.C. Krebs, K. Norrman, New insights into the mechanisms of photodegradation/stabilization of P3HT:PCBM active layers using poly(3-hexyl-d13- Thiophene), Chem. Mater., 25 (2013) 4522-4528.
[14] B. Arredondo, B. Romero, M.J. Beliatis, G. del Pozo, D. Martín-Martín, J.C. Blakesley, G. Dibb, F.C. Krebs, S.A. Gevorgyan, F.A. Castro, Analysing impact of oxygen and water exposure on roll-coated organic solar cell performance using impedance spectroscopy, Solar Energy Materials and Solar Cells, 176 (2018) 397-404.
[15] C. Wang, S. Ni, S. Braun, M. Fahlman, X. Liu, Effects of water vapor and oxygen on non-fullerene small molecule acceptors, Journal of Materials Chemistry C, 7 (2019) 879-886.
[16] C.H. Peters, I.T. Sachs-Quintana, J.P. Kastrop, S. Beaupré, M. Leclerc, M.D. McGehee, High efficiency polymer solar cells with long operating lifetimes, Adv. Energy Mater., 1 (2011) 491-494.
[17] J.G. Sánchez, V.S. Balderrama, M. Estrada, E. Osorio, J. Ferré-Borrull, L.F. Marsal, J. Pallarès, Stability study of high efficiency polymer solar cells using TiOx as electron transport layer, Solar Energy, 150 (2017) 147-155.

[18] V. Turkovic, S. Engmann, D.A.M. Egbe, M. Himmerlich, S. Krischok, G. Gobsch, H. Hoppe, Multiple stress degradation analysis of the active layer in organic photovoltaics, Sol. Energy Mater. Sol. Cells, 120 (2014) 654-668.
[19] W.R. Mateker, M.D. McGehee, Progress in Understanding Degradation Mechanisms and Improving Stability in Organic Photovoltaics, Adv Mater., 29 (2017) 1-16.
[20] D. Bartesaghi, G. Ye, R.C. Chiechi, L.J.A. Koster, Compatibility of PTB7 and PC71BM as a key factor for the stability of PTB7:PC71BM solar cells, Adv. Energy Mater., 6 (2016) 1502338.
[21] J. Schafferhans, A. Baumann, A. Wagenpfahl, C. Deibel, V. Dyakonov, Oxygen doping of P3HT:PCBM blends: Influence on trap states, charge carrier mobility and solar cell performance, Organic Electronics, 11 (2010) 1693-1700.
[22] F.C. Krebs, K. Norrman, Analysis of the Failure Mechanism for a Stable Organic Photovoltaic During 10 000 h of Testing, Prog. Photovoltaics, 15 (2007) 697-712.
[23] G.L. Graff, R.E. Williford, P.E. Burrows, Mechanisms of vapor permeation through multilayer barrier films: Lag time versus equilibrium permeation, J. Appl. Phys., 96 (2004) 1840-1849.
[24] S.R. Dupont, E. Voroshazi, P. Heremans, R.H. Dauskardt, The effect of anneal, solar irradiation and humidity on the adhesion/cohesion properties of P3HT: PCBM based inverted polymer solar cells, 38th IEEE Photovoltaic Specialists Conference , Austin, TX, Art. No, 6318272 (2012) 3259-3262.
[25] A. Guerrero, G. Garcia-Belmonte, Recent Advances to Understand Morphology Stability of Organic Photovoltaics, Nanomicro Lett, 9 (2017) 10.
[26] I.T. Sachs-Quintana, T. Heumüller, W.R. Mateker, D.E. Orozco, R. Cheacharoen, S. Sweetnam, C.J. Brabec, M.D. McGehee, Electron Barrier Formation at the Organic-Back Contact Interface is the First Step in Thermal Degradation of Polymer Solar Cells, Advanced Functional Materials, 24 (2014) 3978-3985.
[27] B. Park, Y.J. Kim, S. Graham, E. Reichmanis, Study of Conformational Change of P3HT Chains Using In-Situ Polarized Raman Spectroscopy, ACS Appl. Mater. Interfaces, 3 (2011) 3545-3551.
[28] M.S. Weaver, L.A. Michalski, K. Rajan, M.A. Rothman, J.A. Silvernail, P.E. Burrows, G.L. Graff, M.E. Gross, P.M. Martin, M. Hall, E. Mast, C. Bonham, W. Bennett, M. Zumhoff, Organic light-emitting devices with extended operating lifetimes on plastic substrates, Appl. Phys. Lett., 81 (2002) 2929-2931.
[29] J. Meyer, P. Görrn, F. Bertram, S. Hamwi, T. Winkler, H.-H. Johannes, T. Weimann, P. Hinze, T. Riedl, W. Kowalsky, Al2O3/ZrO2 Nanolaminates as Ultrahigh Gas-Diffusion Barriers—A Strategy for Reliable Encapsulation of Organic Electronics, 21 (2009) 1845-1849.
[30] J. Ahmad, K. Bazaka, L.J. Anderson, R.D. White, M.V. Jacob, Materials and methods for encapsulation of OPV: A review, Renewable and Sustainable Energy Reviews, 27 (2013) 104-117.
[31] S. Cros, R. de Bettignies, S. Berson, S. Bailly, P. Maisse, N. Lemaitre, S. Guillerez, Definition of encapsulation barrier requirements: A method applied to organic solar cells, Solar Energy Materials and Solar Cells, 95 (2011) S65-S69.
[32] F. Machui, M. Hösel, N. Li, G.D. Spyropoulos, T. Ameri, R.R. Søndergaard, M. Jørgensen, A. Scheel, D. Gaiser, K. Kreul, D. Lenssen, M. Legros, N. Lemaitre, M. Vilkman, M. Välimäki, S. Nordman, C.J. Brabec, F.C. Krebs, Cost analysis of roll-to-roll fabricated ITO free single and tandem organic solar modules based on data from manufacture, Energy & Environmental Science, 7 (2014).
[33] K. Ogura, A. Fujii, H. Shiigi, M. Nakayama, T. Tonosaki, Effect of Hygroscopicity of Insulating Unit of Polymer Composites on Their Response to Relative Humidity, Journal of the Electrochemical Society, 147 (2000) 1105-1109.
[34] D. Qin, W. Wang, M. Wang, S. Jin, J. Zhang, The dependence of the cathode architecture on the photoactive layer morphology in bulk-heterojunction polymeric solar cells, Semiconductor Science and Technology, 29 (2014) 125011.
[35] M. O.Reese, S.A. Gevorgyan, M. Jørgensen, E. Bundgaard, S.R. Kurtz, D.S. Ginley, D.C. Olson, M.T. Lloyd, P. Morvillo, E.A. Katz, A. Elschner, O. Haillant, T.R. Currier, V. Shrotriya, M. Hermenau, M. Riede, K.R. Kirov, G. Trimmel, F.C. Krebs, Consensus stability testing protocols for organic photovoltaic materials and devices, Solar Energy Materials and Solar Cells, 95 (2011) 1253-1267.

[36] Gwyddion (2019). "Gwyddion Software." Accessed 07-Jun, 2019, from http://gwyddion.net/download.php.
[37] A.D. Scaccabarozzi, N. Stingelin, Semiconducting: insulating polymer blends for optoelectronic applications-a review of recent advances, J. Mater. Chem. A, 2 (2014) 10818-10824.
[38] M.L. Jones, R. Dyer, N. Clarke, C. Groves, Are hot charge transfer states the primary cause of efficient free-charge generation in polymer:fullerene organic photovoltaic devices? A kinetic Monte Carlo study, Phys. Chem. Chem. Phys., 16 (2014) 20310-20320.
[39] M.M. Mandoc, W. Veurman, L.J.A. Koster, B. de Boer, P.W.M. Blom, Origin of the Reduced Fill Factor and Photocurrent in MDMO-PPV:PCNEPV All-Polymer Solar Cells, 17 (2007) 2167-2173.
[40] C. Groves, J.C. Blakesley, N.C. Greenham, Effect of Charge Trapping on Geminate Recombination and Polymer Solar Cell Performance, Nano Letters, 10 (2010) 1063-1069.
[41] M. Hermenau, M. Riede, K. Leo, S.A. Gevorgyan, F.C. Krebs, K. Norrman, Water and oxygen induced degradation of small molecule organic solar cells, Solar Energy Materials and Solar Cells, 95 (2011) 1268-1277.
[42] S.-C. Luo, H.-H. Chung, E.T. Pashuck, E.P. Douglas, P.H. Holloway, Formation of bubbles on electrical contacts to polymer light-emitting diode devices, Thin Solid Films, 478 (2005) 326-331.
[43] L.-M. Do, M. Oyamada, A. Koike, E.-M. Han, N. Yamamoto, M. Fujihira, Morphological change in the degradation of Al electrode surfaces of electroluminescent devices by fluorescence microscopy and AFM, Thin Solid Films, 273 (1996) 209-213.
[44] N.B. Kotadiya, A. Mondal, P.W.M. Blom, D. Andrienko, G.A.H. Wetzelaer, A window to trap-free charge transport in organic semiconducting thin films, Nat Mater, 18 (2019) 1182-1186.
[45] G. Zuo, M. Linares, T. Upreti, M. Kemerink, General rule for the energy of water-induced traps in organic semiconductors, Nat Mater, 18 (2019) 588-593.
[46] M. Ramuz, L. Bürgi, C. Winnewisser, P. Seitz, High sensitivity organic photodiodes with low dark currents and increased lifetimes, Organic Electronics, 9 (2008) 369-376.
[47] S. Goffri, C. Muller, N. Stingelin-Stutzmann, D.W. Breiby, C.P. Radano, J.W. Andreasen, R. Thompson, R.A.J. Janssen, M.M. Nielsen, P. Smith, H. Sirringhaus, Multicomponent semiconducting polymer systems with low crystallization-induced percolation threshold, Nat. Mater., 5 (2006) 950-956.
[48] N.B. Kotadiya, H. Lu, A. Mondal, Y. Ie, D. Andrienko, P.W.M. Blom, G.-J.A.H. Wetzelaer, Universal strategy for Ohmic hole injection into organic semiconductors with high ionization energies, Nat. Mater., 17 (2018) 329-334.
[49] B.A. Collins, Z. Li, J.R. Tumbleston, E. Gann, C.R. McNeill, H. Ade, Absolute Measurement of Domain Composition and Nanoscale Size Distribution Explains Performance in PTB7:PC71BM Solar Cells, Advanced Energy Materials, 3 (2012) 65-74.
[50] Y.Y. Liang, Z. Xu, J.B. Xia, S.T. Tsai, Y. Wu, G. Li, C. Ray, L.P. Yu, For the Bright Future-Bulk Heterojunction Polymer Solar Cells with Power Conversion Efficiency of 7.4%, Adv. Mater., 22 (2010) E135-E138.
[51] J.D. Roehling, D. Baran, J. Sit, T. Kassar, T. Ameri, T. Unruh, C.J. Brabec, A.J. Moulé, Nanoscale Morphology of PTB7 Based Organic Photovoltaics as a Function of Fullerene Size, Sci Rep., 6 (2016) 30915-30926.
[52] J. Kettle, Z. Ding, M. Horie, G.C. Smith, XPS analysis of the chemical degradation of PTB7 polymers for organic photovoltaics, Organic Electronics, 39 (2016) 222-228.
[53] S. Shah, Investigating degradation pathways in organic solar cell materials, Iowa State University PhD Dissertation, 16462 (2018) 1-90.
[54] F. Zhang, Z. Zhuo, J. Zhang, X. Wang, X. Xu, Z. Wang, Y. Xin, J. Wang, J. Wang, W. Tang, Z. Xu, Y. Wang, Influence of PC60BM or PC70BM as electron acceptor on the performance of polymer solar cells, Sol. Energy Mater. Sol. Cells, 97 (2012) 71-77.
[55] N. Chander, E. Jayaraman, M. Rawat, A. Bagui, S.S.K. Iyer, Stability and Reliability of PTB7:PC71BM and PTB7:PC61BM Inverted Organic Solar Cells: A Comparative Study, IEEE JOURNAL OF PHOTOVOLTAICS, 9 (2018) 183-193.

[56] M. Kumano, M. Ide, N. Seiki, Y. Shoji, T. Fukushima, A. Saeki, A ternary blend of a polymer, fullerene, and insulating self-assembling triptycene molecules for organic photovolatics, Journal of Materials Chemistry A, 4 (2016) 18490-18498.
[57] M.R. Hammond, R.J. Kline, A.A. Herzing, L.J. Richter, D.S. Germack, H.-W. Ro, C.L. Soles, D.A. Fischer, T. Xu, L. Yu, M.F. Toney, D.M. DeLongchamp, Molecular Order in High-Efficiency Polymer-Fullerene Bulk Heterojunction Solar Cells, ACS Nano, 5 (2011) 8248-8257.
[58] T. Supasai, V. Amornkitbamrung, C. Thanachayanont, I.M. Tang, T. Sutthibutpong, N. Rujisamphan, Visualizing nanoscale phase morphology for understanding photovoltaic performance of PTB7: PC71BM solar cell, Applied Surface Science, 422 (2017) 509-517.
[59] T.A. Ferenczi, C. Muller, D.D. Bradley, P. Smith, J. Nelson, N. Stingelin, Organic semiconductor:insulator polymer ternary blends for photovoltaics, Adv Mater, 23 (2011) 4093-4097.
[60] J.G. Manion, D. Gao, P.M. Brodersen, D.S. Seferos, Insulating polymer additives in small molecule and polymer photovoltaics: how they are tolerated and their use as potential interlayers, Journal of Materials Chemistry C, 5 (2017) 3315-3322.
[61] L. Ye, Y. Jing, X. Guo, H. Sun, S. Zhang, M. Zhang, L. Huo, J. Hou, Remove the Residual Additives toward Enhanced Efficiency with Higher Reproducibility in Polymer Solar Cells, J. Phys. Chem. C, 117 (2013) 14920−14928.
[62] N. Li, C.J. Brabec, Air-processed polymer tandem solar cells with power conversion efficiency exceeding 10%, Energy Environ. Sci., 8 (2015) 2902-2909.